Composites Part B 232 (2022) 109571

Contents lists available at ScienceDirect

Composites Part B

journal homepage: www.elsevier.com/locate/compositesb

Asymmetric SIS membranes specifically loaded with exosomes through the modification of engineered recombinant peptides for guide bone regeneration

Shiqing Ma [a,1], Yifan Zhao [b,1], Yilin Yang [b,1], Yuzhu Mu [b], Lei Zhang [b], Jinzhe Wu [b], Rui Li [b], Xiaowei Bian [b], Pengfei Wei [c], Wei Jing [c,d], Bo Zhao [c,**], Zihao Liu [b,*], Jiayin Deng [b,***]

[a] Department of Stomatology, The Second Hospital of Tianjin Medical University, Tianjin, 300211, China
[b] School and Hospital of Stomatology, Tianjin Medical University, Tianjin, 300070, China
[c] Beijing Biosis Healing Biological Technology Co., Ltd Co., Ltd, Beijing, 102600, China
[d] Foshan (Southern China) Institute for New Materials, Foshan, 528220, China

ARTICLE INFO

Keywords:
GBR
SIS
Asymmetric membrane
Exosomes
Engineered recombinant peptides

ABSTRACT

Guided bone regeneration (GBR) technology is an effective method for reconstructing bone defects, and barrier membranes are widely used in this process. The objective of this study was to develop a novel asymmetric SIS (small intestinal submucosa) membrane and modify the membrane with exosomes and engineered recombinant peptides. The asymmetric SIS membrane was developed with liquid nitrogen quencher. The engineered recombinant peptides were designed by connecting collagen binding peptides with the exosomal capture peptide CP05 via linker. In vitro experiments demonstrated that the engineered recombinant peptides contributed to promoting the positive effect of exosomes on the osteogenic differentiation of BMSCs. Further mechanistic studies confirmed that the PI3K/Akt signaling pathway is critical in the exosome-induced osteogenic differentiation of BMSCs. Moreover, the asymmetric SIS membrane combining engineered recombinant peptides and exosomes could reconstruct bone defects effectively within 12 weeks. Therefore, the membrane developed in this study has the potential to repair bone defects.

1. Introduction

Trauma, inflammation and tumors are common causes of osseous tissue damage [1]. Guided bone regeneration (GBR) technology is emerging as one of the methods most commonly applied for reconstructing bone defects [2]. GBR technology is based on the application of a barrier membrane that covers an osseous defect and excludes any interference from nonosteogenic tissues in the process of bone healing, while providing a favorable environment for bone regeneration [3,4]. The barrier membrane plays a key role in the application of GBR technology.

The majority of recent studies have focused on the construction of bionic layered membranes with an asymmetric structure to meet the different functional needs of the target [5,6]. The dense layer towards the soft tissue acts as a barrier to prevent fibroblasts from invading bone defects. The porous layer facing bone defects possesses high porosity, which can facilitate osteoblast adhesion and the stabilization of blood clots [7,8]. To our knowledge, the Bio-Gide membrane has been used in clinical practice and has achieved effective therapeutic results [9,10]. However, due to its single composition, the Biogide membrane lacks bioactive compounds for inducing bone regeneration. Therefore, asymmetric structures and osteoinductive capabilities are of great significance for absorbable GBR membranes.

Extracellular matrix (ECM) materials have recently become an endearing scaffold material for tissue engineering technology due to their noncellular biological network [11]. Small intestinal submucosa (SIS) is a classical ECM material with low immunogenicity, excellent mechanical properties and tissue regeneration ability [12,13]. Thus, SIS

* Corresponding author.
** Corresponding author.
*** Corresponding author.
E-mail addresses: zhaobo@biosishealing.com (B. Zhao), liuzihao@tmu.edu.cn (Z. Liu), jdeng@tmu.edu.cn (J. Deng).
[1] Shiqing Ma,Yifan Zhao and Yilin Yang contributed equally to this research.

https://doi.org/10.1016/j.compositesb.2021.109571
Received 20 June 2021; Received in revised form 30 November 2021; Accepted 8 December 2021
Available online 26 December 2021

patches are widely used in the repair of damaged tissues, such as skin, cardiovascular, abdominal wall, and cartilage defects, and have achieved satisfactory results [14–16]. However, because SIS patches have a compact texture without a porous structure that provides an appropriate space for bone cells to grow, only a few studies have applied SIS material as a GBR membrane [17]. To obtain an asymmetric structure of the GBR membrane, an improved preparation craft technique should be introduced for modification of the SIS material.

The main techniques used for fabricating asymmetric membranes include phase inversion and electrospinning [18]. As a classical phase inversion technology, liquid nitrogen quencher is commonly used due to its simple operation and avoidance organic applications. Recently, some scholars have successfully developed asymmetric chitosan membranes for healing and guiding bone tissue regeneration using liquid nitrogen quencher, and such membranes exhibit excellent mechanical properties and porosity [19]. Consequently, liquid nitrogen quencher is a promising method for inverting the phase of the SIS membrane to generate a loose and porous structure.

In addition to its asymmetric structure, the osteoinductive capability of the GBR membrane is also essential because it stimulates the differential of multifunctional mesenchymal cells into osteoblasts and thereby creates a suitable microenvironment for the regeneration of osseous tissue. As extracellular vesicles, exosomes act as a cell-to-cell communicator through the transfer of mRNAs, miRNAs and proteins, which are promising therapeutics in the field of bone tissue engineering [20,21]. Moreover, due to their natural origin, high cellular uptake and low immunogenicity, exosomes might provide a novel strategy for promoting MSC activity on biomaterial surfaces [22,23]. The biochemical cues encapsulated in exosomes might induce osteogenesis *in vitro* and *in vivo*. Thus, enhancing the osteogenicity of the SIS membrane by exosomes loading could be an effective attempt. An effective specific binding strategy to increase the loading rate of exosomes is also needed.

Engineered recombinant peptides are nanomolecules constructed by connecting two or more functional peptides through recombinant technology. Due to their low cytotoxicity and small molecular weight, engineered peptides are less likely to induce an immune response [24]. In previous studies, engineered antibacterial peptides have been constructed and used for the surface modification of dental titanium implants [30]. To achieve the specific binding of exosomes to the SIS membrane by bridging engineered recombinant peptides, it is necessary to find the target peptides that can specifically bind to SIS membrane and the functional peptides that can recruit exosomes.

Screened by phage surface display technology, LRELHLNNN or DARKESVQK are capable binding to type I or III collagen, respectively [25,26]. These characteristics exactly coincide with the main composition of the SIS membrane [27,28]. The peptide CP05 (CRHSQMTVTSRL), which can recruit and capture exosomes from various tissue sources, was recently identified by phage display technology [29]. CP05 can specifically bind to the second extracellular loop of CD63, which is a tetrameric protein typically enriched on the surface of exosomes and can thus target and capture exosomes. Consequently, the construction of engineered recombinant peptides by linking CP05 and collagen binding peptides is expected to achieve the specific loading of exosomes on the SIS membrane.

In this study, we aimed to develop an asymmetric SIS membrane using liquid nitrogen quencher and modify the membrane with exosomes by engineered recombinant peptides (Scheme 1). In addition, *in vivo* and *in vitro* experiments were performed to investigate the effect of the engineered recombinant peptides on exosomes in promoting the biological behavior of BMSCs. The asymmetric SIS membrane modified with engineered recombinant peptides and exosomes might serve as a promising GBR membrane for repairing bone defects.

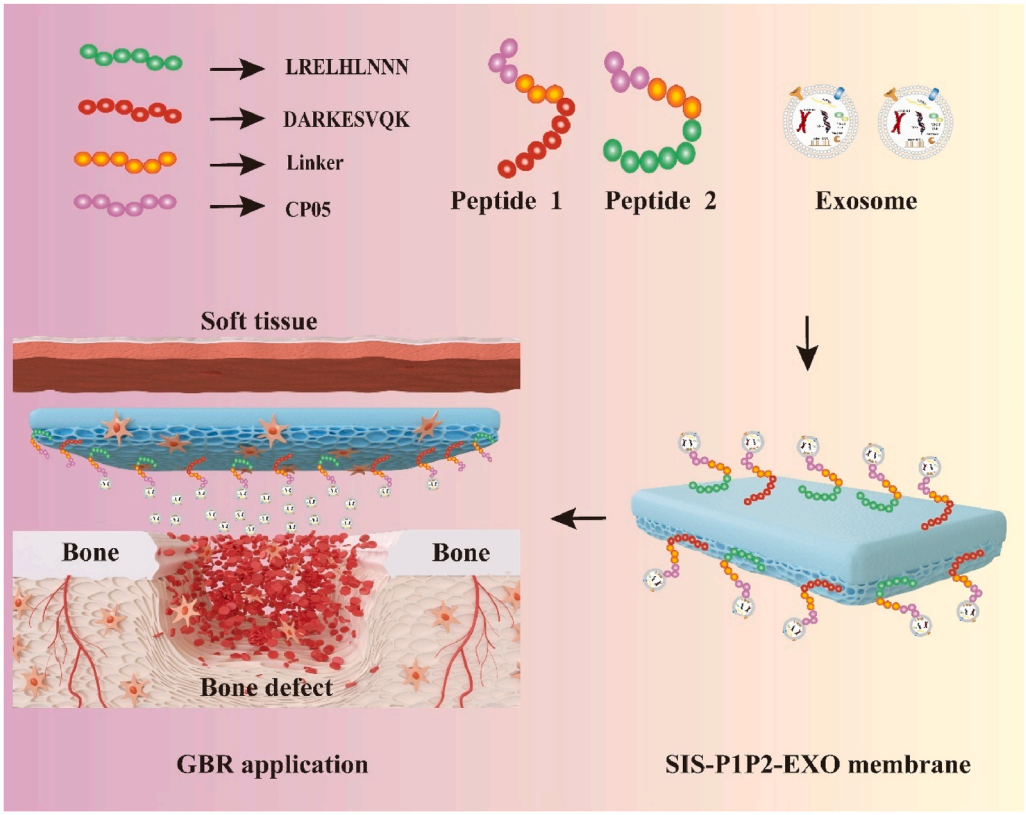

Scheme 1. Schematic illustration of the preparation of the SIS–P1P2-EXO membrane for guiding bone regeneration.

2. Results and discussion

2.1. Design and structural prediction of the engineered recombinant peptides

The predicted pseudo 3D architectures of the engineered recombinant peptides are shown in Fig. 1. The two engineered recombinant peptides were composed of three parts: CP05 (CRHSQMTVTSRL), collagen-binding peptide (type I collagen: DARKESVQK or type III collagen: LRELHLNNN) and linker (PAPAP). The prediction diagram showed that the spatial structures of the engineered recombinant peptides are different (Fig. 1). The backbone structure of P1 was relatively compact because the α-helical structure was rich in hydrogen bonds. P2 had a random coil structure and better mobility, which allowed CP05 to swing over a wider range.

In this study, Pro-rich linker (PAPAP) was selected as the linker for constructing engineered recombinant peptides. Linkers are an essential factor for the construction of engineered recombinant peptides to provide structural flexibility and maintain the original structure of the functional domains [30]. Pro-rich linker (PAPAP), one of the rigid linkers, has been successfully applied to preserve a fixed distance between the domains and to maintain their independent functions, which is useful for the construction of engineered recombinant peptides. The nonhelical rigid linker (PAPAP) exhibits sufficient rigidity and serves to reduce interdomain interference due to Pro-rich sequences, which impose strong conformational constrain and increase the stiffness of the linker [31]. Furthermore, to achieve appropriate separation of the functional domains and avoid mutual interference [32], the sequence of the linker was repeated twice, which might help for engineered recombinant peptides recruit exosomes and anchor the exosomes to the surface of the SIS membrane.

2.2. Morphology of the asymmetric SIS membrane

The asymmetric structure of the SIS membrane was developed through liquid nitrogen quencher. This process results in a temperature gradient between the upper and lower layers of the SIS membrane. It has been proven that the number of crystal nuclei that initially formed at higher temperature is lower than that the number that forms at a lower freezing temperature [33]. Therefore, fewer ice crystal nuclei formed in the upper layer of the SIS membrane, and more ice crystal nuclei formed in the lower layer. This difference in the number of ice crystal nuclei led to larger pores in the upper layer (loose layer) and smaller pores in the lower layer (dense layer) after lyophilization (Fig. 2).

The surface morphology of the asymmetric SIS membrane was characterized by SEM images. As shown in Fig. 2C and F, the cross-section of the SIS membrane presented an asymmetric structure, which included a dense layer and a loose layer, and the surface morphology of the two layers are shown in Fig. 2A, B, D and E, respectively. The dense layer showed a compact and flat surface morphology. The loose layer had large pores that interconnected with each other. The photos of asymmetric SIS membrane were shown in Fig. S1.These results indicate that the asymmetric SIS membrane was successfully developed.

Sufficient mechanical properties are crucial for maintaining the space for bone formation. The tensile strength of the membranes at dried and wetted was shown in Fig. S2. The SIS, SIS-EXO and SIS–P1P2-EXO membrans group presented approximate tensile strength to that of Biogide. There was no significant difference between the groups. The tensile strength of all groups decreased slightly at wetted conditions, which may be due to the degradation of collagen.

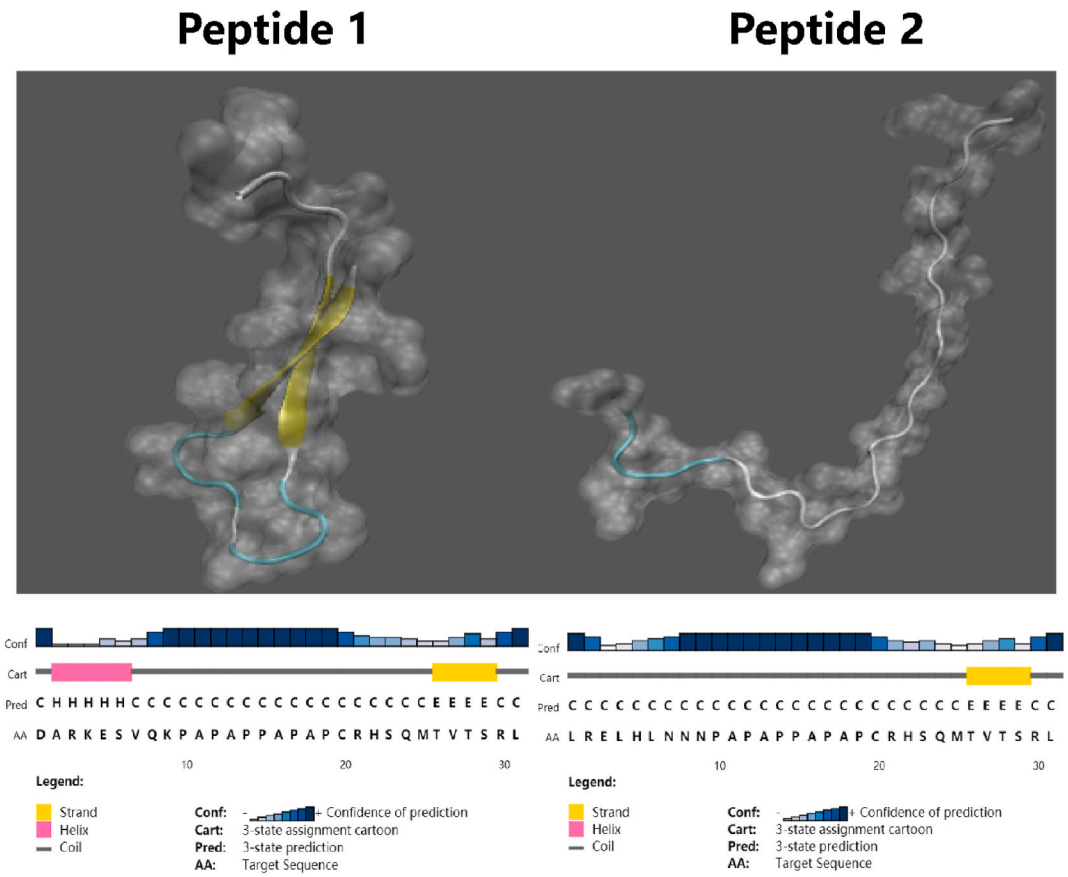

Fig. 1. Pesudo-3D views of the molecular architectures visualized by VMD. The tertiary structures of Peptide 1 and Peptide 2 were predicted by protein analysis software Robetta and visualized by VMD. P1: DARKESVQKPAPAPPAPAPCRHSQMTVTSRL; P2: LRELHLNNNPAPAPPAPAPCRHSQMTVTSRL.

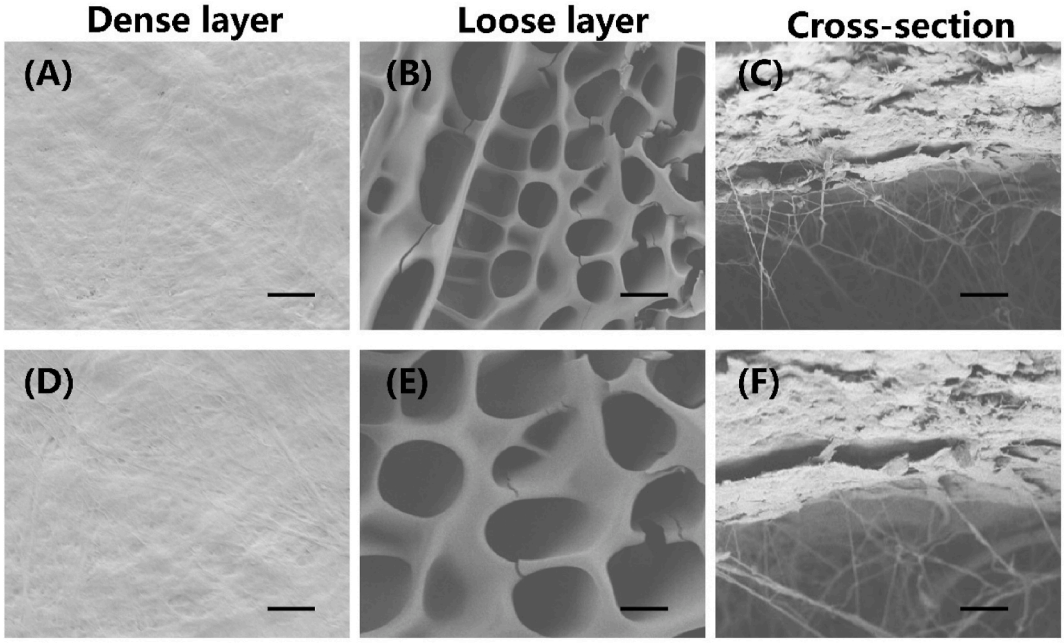

Fig. 2. SEM photographs showing the morphologies of an asymmetric porous SIS membrane: (**A**) dense layer (× 1000); (**B**) loose layer (× 1000); (**C**) cross-section (× 1000); (**D**) dense layer (× 2000); (**E**) loose layer (× 2000); and (**F**) cross-section (× 2000). Low magnification scale bar:40 μm. High magnification scale bar:20 μm.

2.3. Characterization of exosomes and modified asymmetric SIS membrane surfaces

Exosomes were extracted from the culture medium of BMSCs by centrifugation. TEM, NTA analysis and Western blotting were used to characterize the exosomes derived from BMSCs. The results showed that the majority of these particles exhibited a cup- or round-shaped morphology with a size ranging from 50 to 150 nm (Fig. 3A and B), which suggested the presence of exosomes. Western blotting analysis (Fig. 3C) showed that the exosomes characteristic surface markers CD63, CD9, CD81and Alix were positive and Cytochrome C (cell marker) was negative. These results suggested that the exosomes were successfully isolated.

The concentration screening pre-experiment was also carried out. The SIS membranes were soaked in different concentrations of peptides solutions to observe the binding ability of engineered recombinant peptides. CLSM images (Fig. S3) showed that P1 and P2 could achieve good binding effect with SIS membrane at 200×10^{-6} M. The exosome particles distributed on the surfaces of the SIS-EXO and SIS–P1P2-EXO membranes exhibited a cup-shaped morphology with a heterogeneous size (Fig. 3D). To further demonstrate whether the exosomes and engineered recombinant peptides were modified on the SIS membrane, a group of CLSM images verified the loading of the exosomes and engineered recombinant peptides (Fig. 3E). The CLSM images showed that DiR-labeled exosomes (purple particles) were homogeneously distributed on the SIS–P1P2-EXO membrane, and only scattered purple particles were found on the SIS membrane (Fig. 3E). There were more DIR-labeled exosomes on the SIS–P1P2-EXO membrane than on the SIS-EXO membrane, demonstrating the effective recruitment of engineered recombinant peptides.

To further clarify the release of engineered recombinant peptides and exosomes, changes in engineered recombinant peptides and exosomes on the SIS–P1P2-EXO membrane were observed by CLSM (Fig. S4). On the first day, a large number of engineered recombinant peptides and exosomes could be observed on the SIS–P1P2-EXO membrane. With the extension of time, the engineered recombinant peptides and exosomes bound on the surface of SIS–P1P2-EXO membrane decreased. After 10 day, the content of engineered recombinant peptides and exosomes decreased significantly, but it still could be observed on SIS–P1P2-EXO membrane, indicating engineered recombinant peptides and exosomes could maintain for a certain time and release continuously.

Taken together, these results implied that the exosome- and engineered recombinant peptides-modified SIS membrane was successfully developed. The desirable modification effect of the engineered recombinant peptides on the SIS membrane might ascribed to the linker (PAPAP), which served as a passive linker to maintain a distance between the collagen binding peptide and CP05 and resulted in engineered recombinant peptides with a higher structural stability. Further *in vitro* experiments will assess whether the SIS–P1P2-EXO membrane has a more positive influence on cell behaviors than the SIS-EXO membrane.

2.4. Internalization of exosomes by BMSCs and effect of exosomes on cell proliferation

Accumulating evidence suggests that exosomes can regulate the tissue repair course by stimulating cell proliferation and differentiation [34]. To prove that exosomes can be taken up by cells and have an effect on cell behaviors, BMSCs were incubated with DiI-labeled exosomes for 8 h, 12 h, 24 h, 48 h and 72 h, respectively. Fluorescence microscopy images showed that the exosomes (red granules) were gradually internalized by the BMSCs from 8 h to 24 h (Fig. 4A). After 48 h of incubation, a large number of exosomes were internalized and distributed in the perinuclear region (Fig. 4A). The fluorescence intensity reached a peak at 72 h, demonstrating that exosomes could be transported to recipient cells to regulate cell behaviors in the prophase of tissue repair.

A CCK-8 assay was performed to assess cell proliferation over a period of 7 days (Fig. 4B). The OD value of the exosome-treated group was significantly higher than those of the blank and SIS groups ($p < 0.05$). The SIS–P1P2-EXO group showed greater proliferation of BMSCs than the SIS-EXO group ($p < 0.05$), and no statistical differences were found between the blank and SIS groups ($p > 0.05$).

The above results indicate that the engineered recombinant peptides could enhance the retention and stability of exosomes and strengthened the therapeutic effect. The SIS membrane modified by the engineered recombinant peptides and exosomes possesses ideal biocompatibility and exhibits a stronger ability to promote cell activities, which indicates

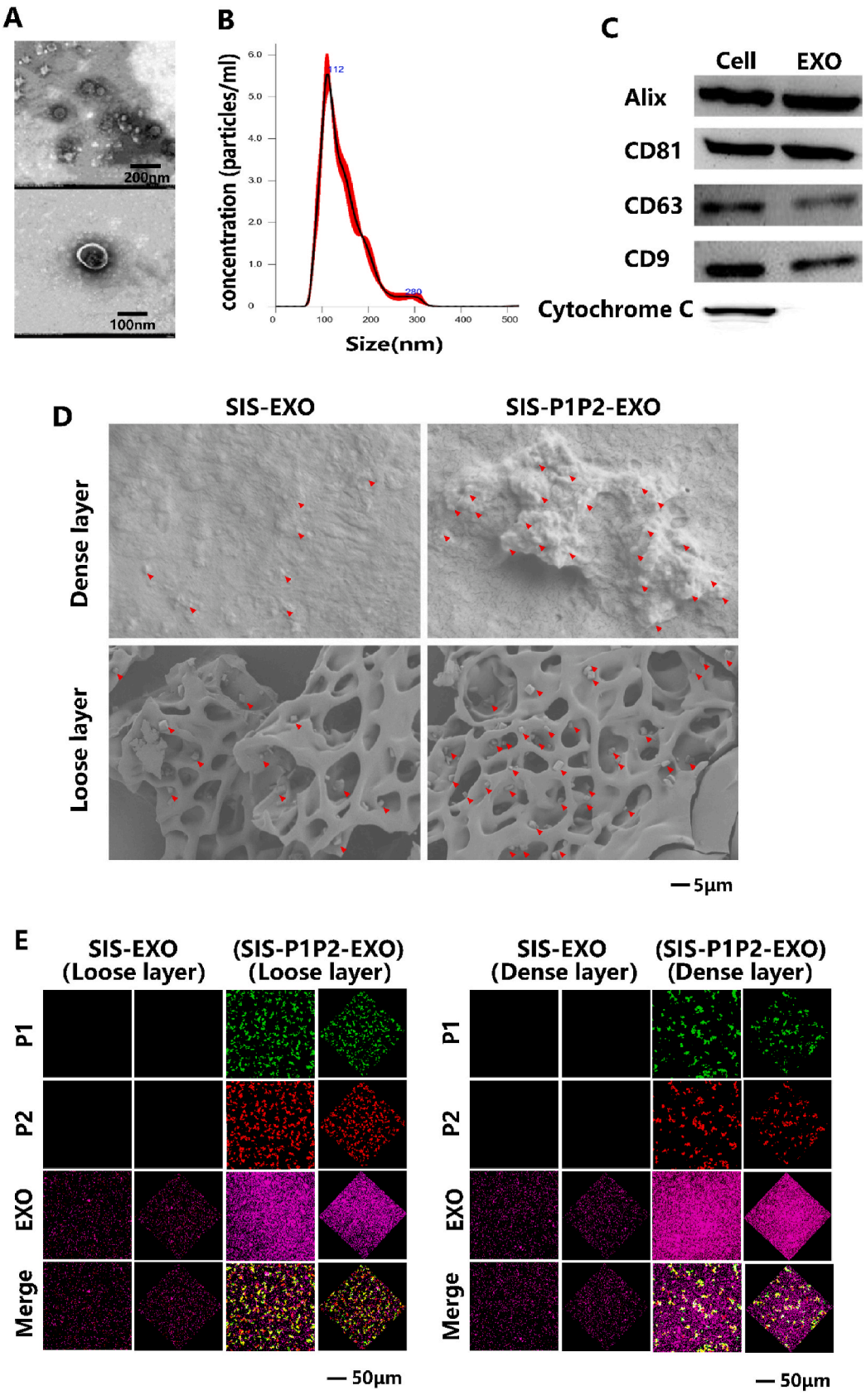

Fig. 3. Characterization of exosomes and modified asymmetric SIS membrane surfaces. (**A**) Morphology of exosomes observed by TEM. (**B**) Particle size distribution of exosomes measured by NanoSight analysis. (**C**) Western blotting analysis of exosomal surface markers (CD63, CD81, Alix and CD9). The cells were stained with Cytochrome *c*. (**D**) SEM images of SIS membranes modified with exosomes (SIS-EXO membranes), SIS membrane modified by engineered recombinant peptides and exosomes (SIS–P1P2-EXO membranes). (**E**) Distribution of DiR-labeled exosomes on the SIS-EXO and SIS–P1P2-EXO membrane surfaces. P1 was labeled with FITC (green), and P2 was labeled with RhodaminB (red). High magnification scale bar: 50 μm. (For interpretation of the references to colour in this figure legend, the reader is referred to the Web version of this article.)

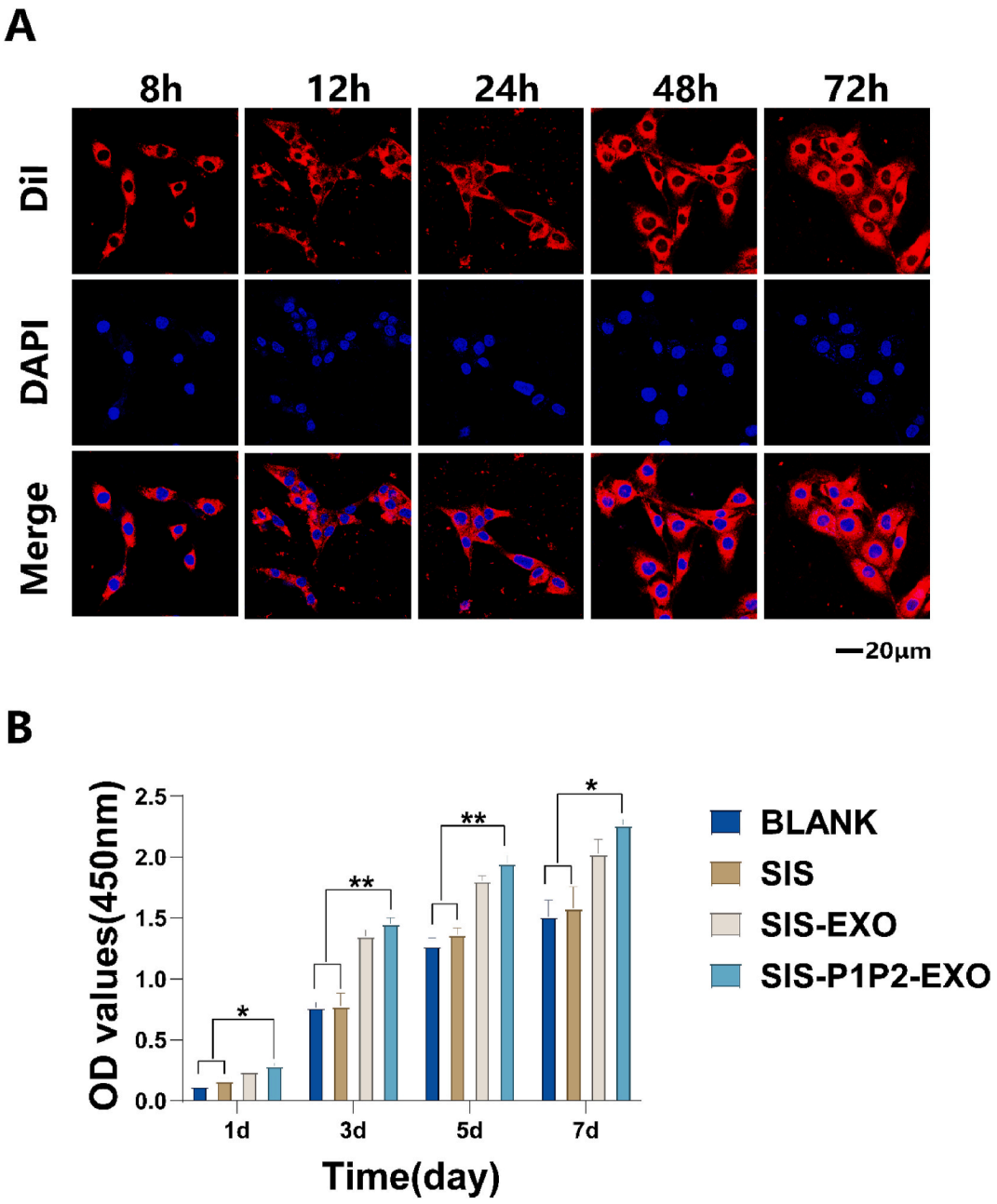

Fig. 4. Internalization of exosomes by BMSCs and biocompatibility of SIS, SIS-EXO and SIS–P1P2-EXO *in vitro*. (**A**) BMSCs were incubated with DiI labeled exosomes (red) for 8 h, 12 h, 24 h, 48 h and 72 h. The nucleus of BMSCs were stained with DAPI (blue). (**B**) Proliferation ability of BMSCs by CCK-8 analysis. *$p < 0.05$;**$p < 0.01$. (For interpretation of the references to colour in this figure legend, the reader is referred to the Web version of this article.)

that the engineered recombinant peptides have potential applications in biomaterial modification.

2.5. SIS membranes modified with the engineered recombinant peptides and exosomes promote the osteogenic differentiation of BMSCs

The osteogenic differentiation of BMSCs is regulated by factors such as BMP2, OCN, ALP and OPN [35]. In this study, Western blot analysis revealed that BMP2, OCN, ALP and OPN expression levels were significantly upregulated in the BMSCs of the SIS–P1P2-EXO and SIS-EXO compared with those of the SIS and blank group ($p < 0.05$) (Fig. 5A). The upregulation of osteogenesis-related marker expression at the protein level was further confirmed by immunofluorescence (Fig. 5C). IF staining demonstrated that the SIS–P1P2-EXO and SIS-EXO groups showed a significant increase in the fluorescence intensity of BMP2, OCN, ALP and OPN. Among the groups, the SIS–P1P2-EXO group displayed the highest expression levels of osteogenesis-related protein markers. The related expression levels of mRNAs were confirmed by qRT-PCR analysis (Fig. 5B). Consistently, the qRT-PCR analysis showed that the SIS–P1P2-EXO group exhibited the highest mRNA levels of BMP2, OCN, ALP and OPN ($p < 0.05$). In conclusion, the SIS–P1P2-EXO membrane significantly contributed to the osteogenic differentiation of BMSCs.

Cell-material interactions and cell-cell communication, which involve multiple cell-secreted signaling factors, are major biological processes during bone healing and remodeling [36]. The design of GBR membranes that can provide an osteogenic microenvironment to induce osteogenic differentiation of BMSCs is of great significance for bone tissue regeneration. In this study, exosomes released from the SIS–P1-P2-EXO membrane at the early stage were helpful for the regulation of

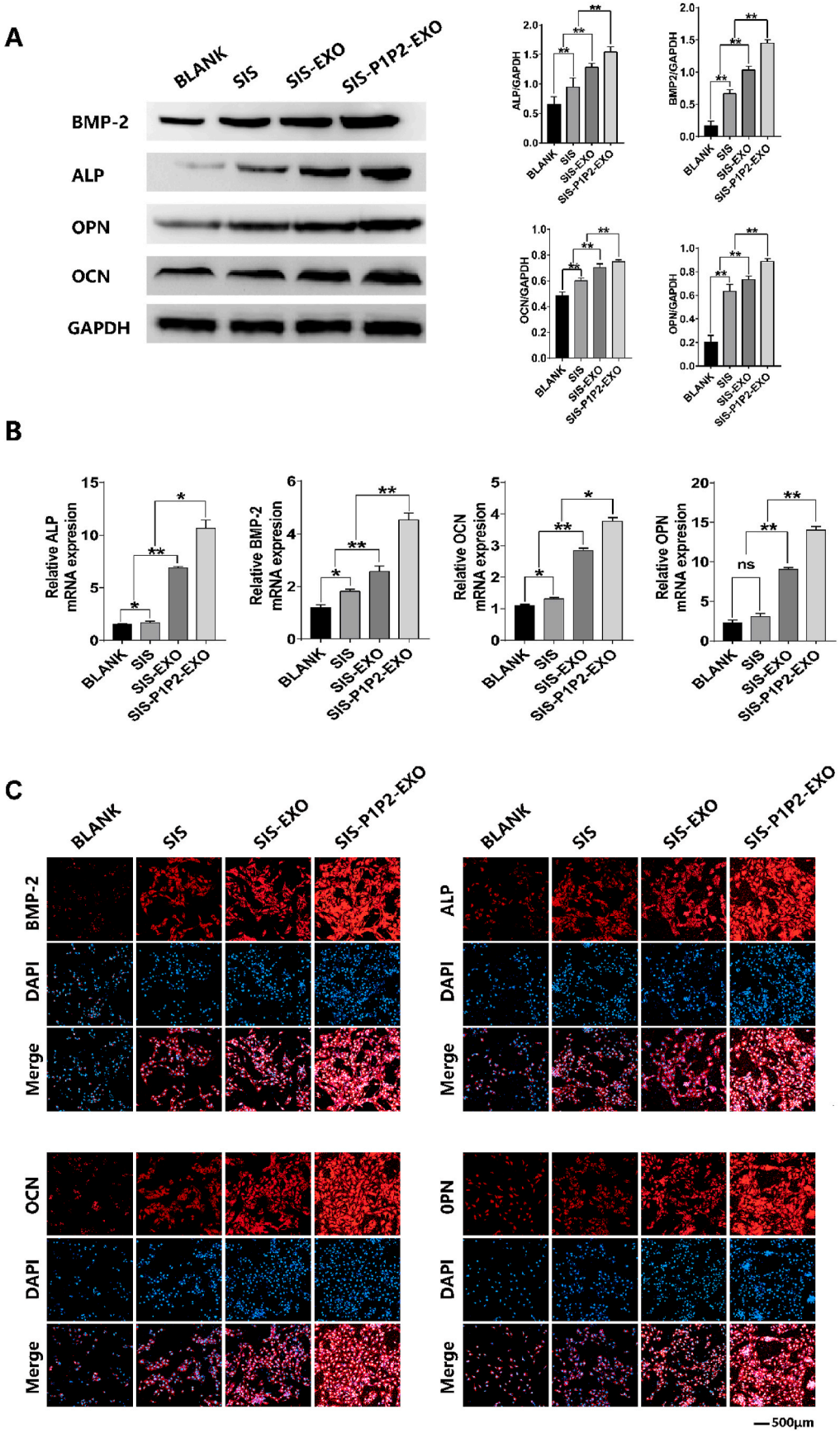

Fig. 5. Effects of the SIS–P1P2-EXO, SIS-EXO, SIS and blank groups on the osteogenic differentiation of BMSCs. (**A**) The protein expression levels of BMP2, OCN, ALP and OPN were determined by Western blotting. The protein levels were quantitated by densitometry and nomarlized to the level of GAPDH. (**B**) RNA expression of osteogenesis-related genes (BMP2, OCN, ALP and OPN). *p < 0.05; **p < 0.01. (**C**) Representative immunofluorescence staining of osteogenic markers (BMP2, OCN, ALP and OPN). BMP2, OCN, ALP and OPN are shown in red and nuclei in blue, stained with DAPI. (For interpretation of the references to colour in this figure legend, the reader is referred to the Web version of this article.)

intercellular communication and ultimately for the activation of a cascade of cell responses. The SIS–P1P2-EXO membrane exhibited higher osteogenic capacity than the SIS-EXO membrane, which indicated that the engineered recombinant peptides exerted a positive effect on exosomes-mediated promotion of the osteogenic differentiation of BMSCs.

2.6. Activation of the PI3K/Akt signaling pathway

We further clarified the molecular mechanisms of exosomes on the osteogenic differentiation of BMSCs. Research has shown that exosomes secreted by human BMSCs can activate several signaling pathways (including Akt, Erk1/2 and STAT3) targeting MSCs and increase their osteogenic differentiation [37]. In particular, the PI3K/Akt signaling pathway has been reported to play important roles in osteogenic

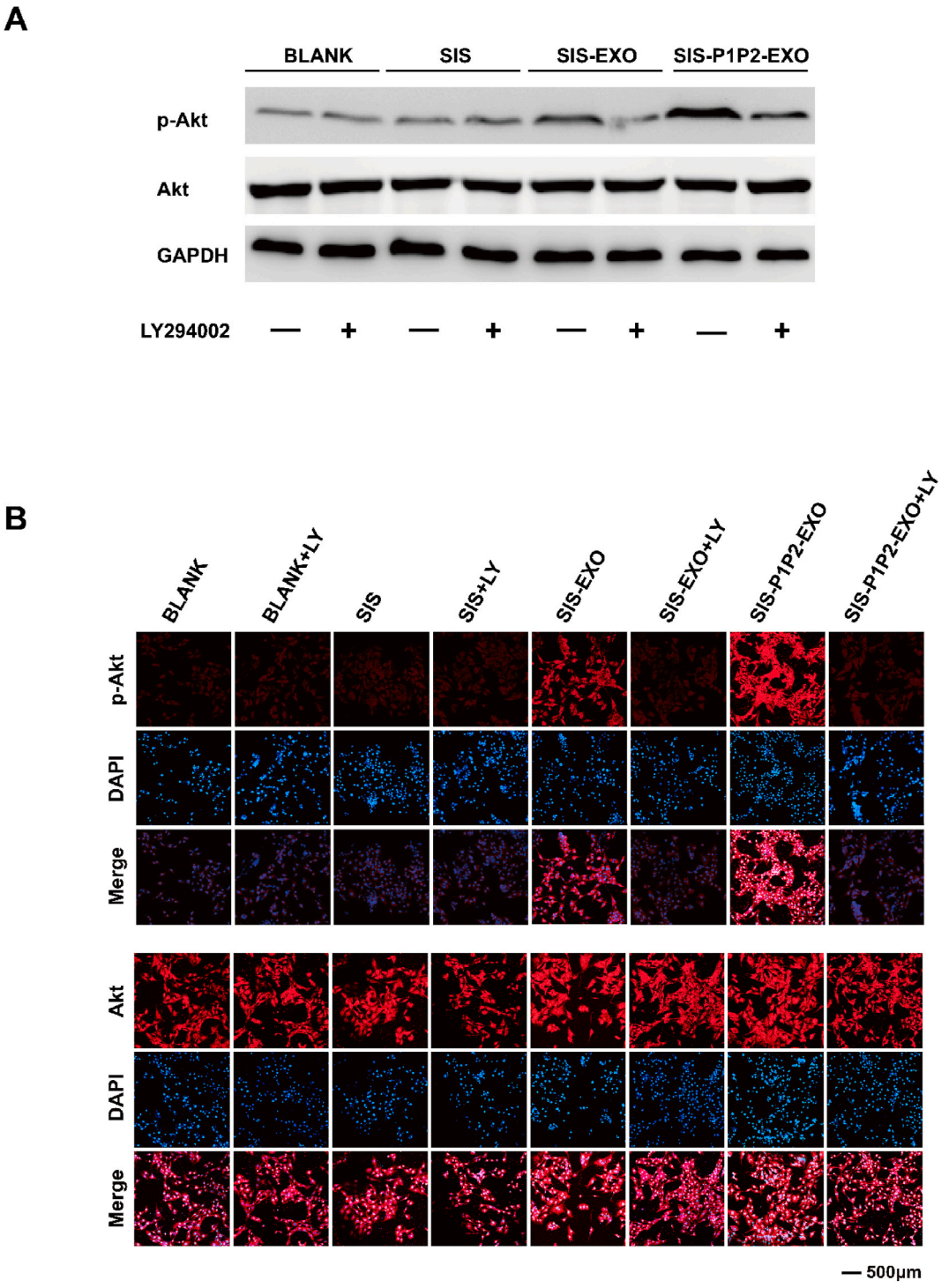

Fig. 6. Exosomes induced the activation of the PI3K/Akt signaling pathway, and these effects were abolished by a PI3K inhibitor (LY294002). (**A**) Western blot for p-Akt and total Akt in BMSCs cultured for 5 days. GAPDH expression was used as a normalization control. (**B**) Immunofluorescence staining for p-Akt and total Akt in BMSCs cultured for 5 days. Phospho-Akt (p-Akt) and total Akt are shown in red, and nuclei are shown in blue. (For interpretation of the references to colour in this figure legend, the reader is referred to the Web version of this article.)

differentiation of BMSCs and bone regeneration [38]. To observe the effects of exosomes on PI3K/Akt pathway, we examined Akt and p-Akt levels using WB and IF assays (Fig. 6A and B). The p-Akt levels were gerater on SIS–P1P2-EXO and SIS-EXO group than on SIS and blank group. The SIS–P1P2-EXO group exhibited the highest level of p-Akt may because of a large number of exosomes were captured by the engineered recombinant peptides. However, the upregulation of p-Akt in BMSCs by exosomes was suppressed by the culture of the BMSCs with a PI3K inhibitor (LY294002). None of the treatments altered the expression level of total Akt. These results indicated that the PI3K/Akt signaling pathway in BMSCs is activated by exosomes. The osteogenic differentiation of BMSCs induced by exosomes is at least partially due to activation of the PI3K/Akt signaling pathway.

2.7. Evaluation of the bone regeneration ability of the SIS–P1P2-EXO membrane in vivo

To investigate the therapeutic potential of the SIS–P1P2-EXO membrane on bone defect repair, critical size defects with a diameter of 8 mm were created in animal experiments, and the membrane was implanted into the defect area. As shown in Fig. 7A, micro-CT images of the all groups showed that the formation of new bone developed from the defect edge to the center. The defect was filled with homogeneous mature bone when covered with the SIS–P1P2-EXO membrane (Fig. 7A). In particular, the surface morphology of the healed defects closely resembled that of surrounding normal bone. Although some bone fragments were found in the Biogide and SIS-EXO groups, the boundary between the defects and the surrounding normal bone was still visible. In the control and SIS groups, only small numbers of highly dense spots were observed. Moreover, 3D reconstruction was conducted through the analysis of the bone volume fraction (BV/TV) and the bone mineral density (BMD) (Fig. 7B and C). Quantification of the micro-CT images provided further evidence that significantly more new bone was formed in the SIS–P1P2-EXO group than in the other four groups ($p < 0.05$). The representative micro-CT images and quantitative analysis suggest that the SIS–P1P2-EXO membrane effectively activates the bone tissue repair process.

2.8. Histological assessment of the bone regeneration ability of the SIS–P1P2-EXO membrane in vivo

A histological analysis was conducted to evaluate the growth of collagen and new tissue as well as the infiltration of lymphocytes. The HE staining results showed no obvious inflammatory tissue in each group. The defect area of the blank group was filled with large fibrous connective tissues, and there were no obvious signs of new bone formation (Fig. 8A). In the SIS group, a small amount of newly formed bone tissue was observed in the center of the defect area. In the SIS-EXO and Biogide groups, the newly trabecular bones were evenly distributed without invasion of fibrous connective tissue. The SIS–P1P2-EXO group showed the best structural integrity among all the groups. The collagen content is closely related to bone formation. Masson-Goldner staining revealed more mature collagen and osteoid tissue formation in the SIS–P1P2-EXO membrane group than in the other groups (Fig. 8B). The early-formed bone was reconstructed into regular lamellar bone, which exhibited red staining in Masson-Goldner staining because of the abundant collagen matrix deposition. IHC staining showed that the SIS-EXO group formed more new bone than the SIS and control groups

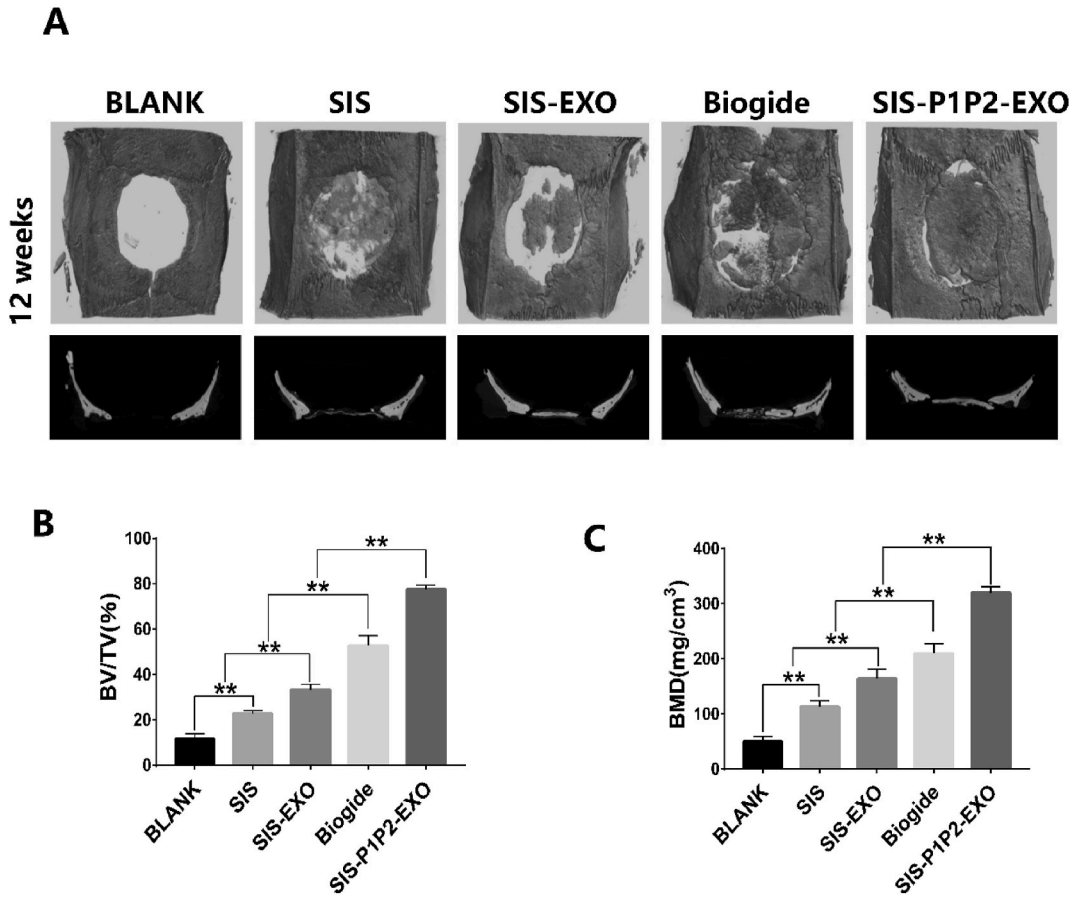

Fig. 7. General evaluation of the *in vivo* performance at 12 weeks after implantation of the SIS, SIS-EXO, Biogide and SIS–P1P2-EXO membranes. (**A**) Representative three-dimensional(3D) reconstruction and sagittal surface images of critical-sized rat calvarial full-thickness defects. Summarized date of the (**B**) bone volume fraction (BV/TV) and (**C**) bone mineral density (BMD) in defect area. *$p < 0.05$; **$p < 0.01$.

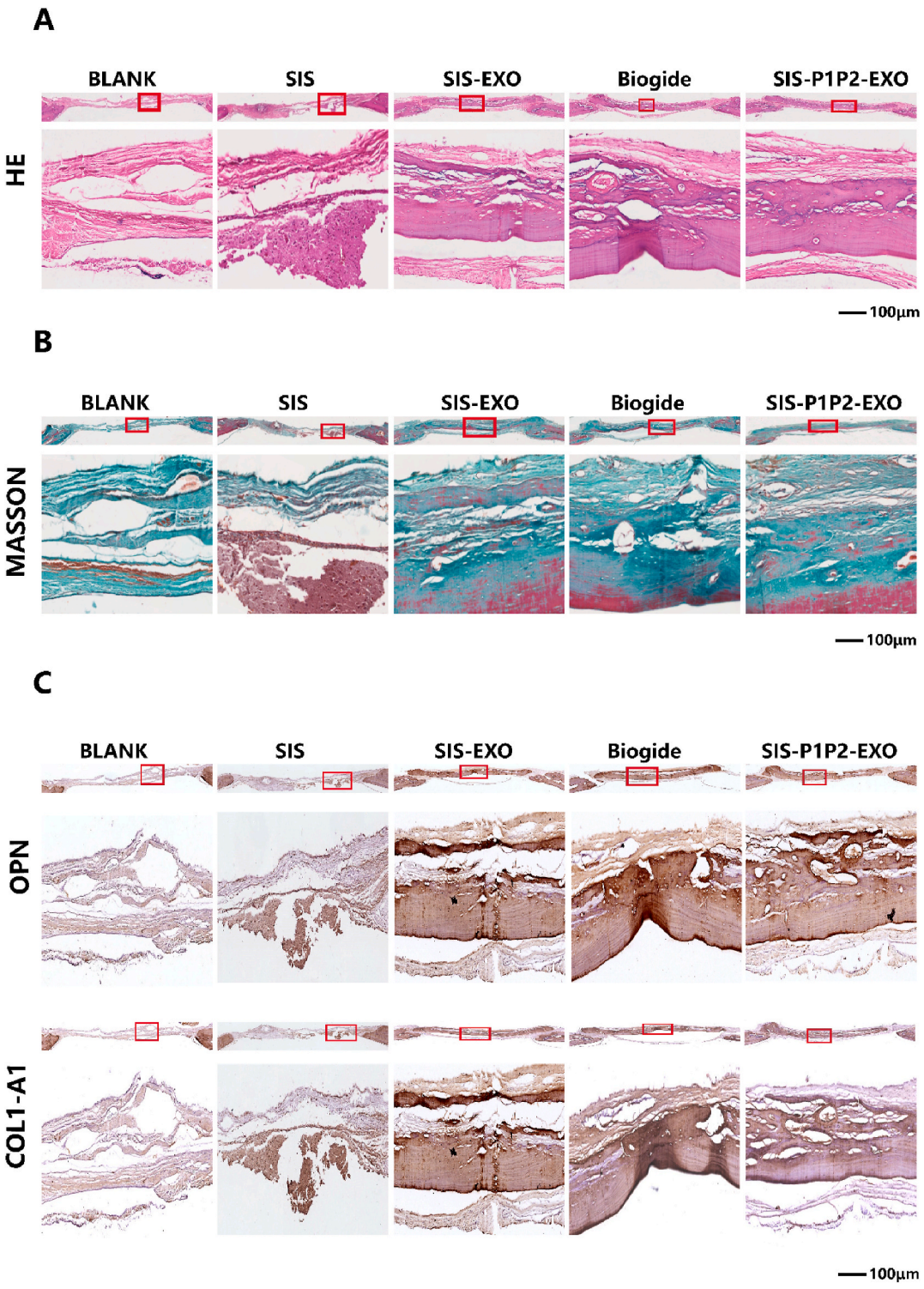

Fig. 8. Histological and immunohistochemical analysis of the newly formed bone at 12 weeks. (**A**) H&E staining of histological sections. (**B**) Masson-Goldner staining of histological sections. (**C**) Immunohistochemical staining for the osteogenic markers COL1-A1 and OPN.

(Fig. 8C). Higher expression of OPN and COL1-A1 was detected in the Biogide group. The highest expression level was found in the SIS–P1P2-EXO group, which suggested that the SIS–P1P2-EXO membrane exerted the strongest effect on bone regeneration.

The above results showed that the SIS–P1P2-EXO membrane could effectively prevent fibrous connective tissue from growing into the defect area and provided space for bone regeneration. The engineered recombinant peptides constructed in this study might prolong the action time of exosomes and improve their stability. The SIS–P1P2-EXO membrane exhibited the strongest bone repair effect because a large number of exosomes were captured by the engineered recombinant peptides. The excellent bone regeneration capability of SIS–P1P2-EXO membrane is helpful to solve the problems of bone loss caused by trauma or inflammation and insufficient alveolar bone mass in the dental implant area. In addition, exosomes-engineered recombinant peptides provides a new therapeutic idea for acellular tissue regeneration.

3. Conclusions

In this study, we developed an asymmetric SIS membrane using liquid nitrogen quencher. The SIS membrane could be specifically combined with BMSC-exosomes through the modification of engineered recombinant peptides. The peptides promote the positive effect of exosomes on the osteogenic differentiation of BMSCs. The SIS–P1P2-EXO membrane could reconstruct bone tissue defects effectively and achieve cell-free bone regeneration within 12 weeks. Furthermore, the PI3K/Akt signaling pathway might play a critical role in the pro-osteogenic effects of the SIS–P1P2-EXO membrane on BMSCs. These results demonstrate that the SIS–P1P2-EXO membrane has the potential for clinical application as a novel GBR membrane.

4. Methods

Synthesis of Engineered Recombinant Peptides: The engineered recombinant peptides were commercially synthesized (Jill Biochemical Shanghai Co., Ltd, China) according to the sequences in Fig. 1, using the Fmoc solid-phase peptide synthesis method. Peptide 1 was labeled with fluorescein isothiocyanate (FITC) and peptide 2 was labeled with rhodamine B (RB). The peptides were purified to at least 90% purity and analyzed by mass spectrometry. The tertiary molecular architectures of the two engineered recombinant peptides were predicted using the protein analysis software Robetta.

Fabrication of the Asymmetric SIS Membrane: The SIS membranes were provided by Beijing Biosis Healing Biological Technology Co., Ltd. The asymmetric structure of the SIS membranes was obtained by immersion in liquid nitrogen for 20s and subsequent lyophilization to produce a porous structure. The membranes were cut into discs with a diameter of 10 mm/35 mm matching the well size of a 24-well/6-well plate and soaked overnight in peptide solution and exosome suspension. Subsequently, the membranes were removed and lyophilized to generate engineered recombinant peptides and exosomes-modified asymmetric SIS membrane. The samples were assigned to the SIS, SIS-EXO and SIS–P1P2-EXO groups.

Mechanical properties: The SIS, SIS-EXO, SIS–P1P2-EXO and Biogide membranes were tailored into proper specimens (15 mm in width, 20 mm in length) for the measurement of tensile strength. The measurement was carried out using ultimate tensile test machine (3367, Instron, USA) with a crosshead speed of 10 mm/min at both wetted (soaking in PBS for 0.5 h in advance) and dried conditions. Then, the tensile strengths of the specimens were calculated and recorded on the basis of a Blue Hill Systems.

Morphological Observation of the Engineered Recombinant Peptides and Exosomes-Modified Asymmetric SIS Membrane: The surface morphology of the SIS and SIS–P1P1-EXO groups was observed by scanning electron microscopy (SEM; Nova NanoSEM 430, FEI, Netherland). Before scanning, the samples were sputter-coated with gold in an argon atmosphere using a sputter coater (K575XD, Emitch, England). A confocal laser scanning microscope (CLSM; FV1000, Olympus, Japan) was used to observe the target binding of the engineered recombinant peptides and exosomes on the surface of SIS membranes.

Cell Culture and Conditioned Medium Collection: Rat bone mesenchymal stem cells (BMSCs, 1×10^5,Cyagen Biosciences, China) were seeded on the SIS, SIS-EXO and SIS–P1P2-EXO membranes and cultured in proliferation medium containing Dulbecco's modified Eagle's medium (DMEM), 10% (v/v) fetal bovine serum (FBS), 100 U/ml penicillin G and 100 mg/ml streptomycin for 7 days. The cultured medium was changed every 3 days.

Exosomal Characterization: Exosomes were isolated from BMSCs by ultracentrifugation. The culture medium of the BMSCs was collected in conical tubes for later using. Several centrifugation and filtration steps were performed for the purification of the exosomes. Briefly, the culture medium was centrifuged at 800 g for 30 min to eliminate dead cells and at 12,000 g for 60 min and was then filtered through a 0.22-μm filter to remove cellular debris. The supernatant was then ultracentrifuged at 100,000 g for 90 min, washed with PBS at 100,000 g for 90 min (Ultracentrifuge, Beckman Coulter, L-90K). The exosome suspension was stored at −80 °C.

Transmission electron microscopy (TEM; Nova Nano TEM 430, Netherland) was used to observe the morphology of exosomes. The concentrated exosomes were fixed with 4% paraformaldehyde for 30 min. Then the mixture was dropped onto carbon coated copper grids and dried for 15 min. The dried mixture was stained twice with 1% uranyl acetate (5 min each). Images were obtained using a TEM at 120 kV. The particle size and distribution of exosomes was measured by nanoparticle tracking analysis (NAT, NanoSight Ltd, Malvern, UK). NTA analytical software (Nanoparticle Tracking Analysis, version 2.3) was used for the analysis. Exosome-specific markers, such as CD63, CD81, CD9 and Alix, were identified by Western blotting.

Assays of the Stability of Engineered Recombinant Peptide and Exosomes: To test the release of engineered recombinant peptide and exosomes, FITC-labeled and RhodaminB-labeled peptides were coated on the SIS membrane surfaces. The peptide-modified SIS membranes were soaked in the exosome suspensions overnight at 4 °C before use. The samples were observed using a confocal laser scanning microscope (CLSM, Nikon Air Confocal, Australia).

Assay of Exosome Uptake: The exosomes were labeled with DiI (Sigma-Aldrich). Briefly, 100 μl of the exosome suspension was mixed with 5 μl DiI for 1 h. The labeled exosomes were then washed in PBS and centrifuged at 100,000 g for 1 h. Afterward, the exosomes were incubated with the BMSCs for 8 h,12 h, 24 h, 48 h and 72 h respectively. After incubation, the cells were washed with PBS, fixed in 4% paraformaldehyde for 30 min and washed again. DAPI solution was used for staining of the nuclei. Images were captured with a CLSM (Nikon Air Confocal, Australia).

Cell Proliferation Assay: The viability of cells was measured by the CCK-8 assay. Briefly, SIS, SIS-EXO and SIS–P1P2-EXO samples were cut into circles with a diameter of 6 mm and placed into a 96-well plate. Subsequently, BMSC cells were seeded in 96-well plates (2000 cells/well). Three replicates were performed for each group. After 1, 3, 5, and 7 d, 10 μl of CCK-8 reagent (Solarbio, China) was added to each well, followed by incubation for 4h at 37 °C. OD value was calculated at 450 nm absorbance.

Quantitative Real-Time Polymerase Chain Reaction (qRT-PCR) Analysis: BMSCs were cultured in osteogenic medium for 7 days. Total RNA was extracted using TRIzol reagent (Invitrogen, USA), and reverse transcription was then performed using GoScript™ Reverse Transcription Mix (Promega, USA). qRT-PCR Kit (Qiagen, Germany) was used to detect the mRNA expression of bone morphogenetic protein-2 (BMP-2), osteocalcin (OCN), alkaline phosphatase (ALP) and osteopontin (OPN). GAPDH was used for reference. The fold differences were calculated using the ΔΔCt method. The primers are listed in Table 1.

Western Blotting Analysis: Three days after 1×10^5 BMSCs were seeded onto six-well plates with the sterilized SIS, SIS-EXO and SIS–P1P2-EXO membranes, the culture medium in the well was replaced by osteoinductive medium. Cell lysates were diluted with protein

Table 1
Primer sequences for real-time PCR.

Gene	Primer sequences (5′–3′)
BMP-2	F: TGCGGTCTCCTAAAGGTCG
	R: ACTCAAACTCGCTGAGGACG
ALP	F: TGACCACCACTCGGGTGAA
	R: GCATCTCATTGTCCGAGTACCA
OCN	F: GGTGCAGACCTAGCAGACACCA
	R: AGGTAGCGCCGGAGTCTATTCA
OPN	F: GTGGTGATCTAGTGGTGCCAAGAGT
	R: AGGCACCGGCCATGTGGCTAT
GAPDH	F: GACGGCCGCATCTTCTTGTGC
	R: TGCAAATGGCAGCCCTGGTGA

loading buffer (4 ×) and heated at 95 °C for 10 min. The protein extracts were separated by sodium dodecyl sulfate-polyacrylamide gel electrophoresis and transferred to polyvinylidene fluoride membranes (Sigma, USA) for 90 min at 300 mA. The membranes were blocked for 1 h with 5% BSA (Sigma, USA) at room temperature and incubated with the primary antibodies (Abcam, UK) at 4 °C overnight. The membranes were then incubated with secondary antibodies (Abcam, UK) at 37 °C for 70 min. The primary antibodies included anti-BMP2 (1:1000, Abcam), anti-OCN (1:1000, Abcam), anti-ALP (1:1000, Abcam), anti-OPN (1:1000, Abcam), anti-p-Akt(1:1000, Abcam) and anti-Akt(1:1000, Abcam). All the values were normalized by GAPDH (1:1000, Abcam).

Immunofluorescence Staining: For immunofluorescence analysis, the cells were fixed with 4% formaldehyde at room temperature for 30 min. After the cells were permeabilized with 0.25% Triton X-100 (Sigma, USA) for 10 min, BMP-2, OCN, ALP, OPN, p-Akt and Akt(Abcam, UK) were then immunostained using the corresponding antibodies. The cells were further labeled with a secondary antibody conjugated with fluorescein isothiocyanate. DAPI was used to stain the nuclei. The cells were then imaged with a CLSM (Nikon Air Confocal, Australia).

PI3K/Akt Signaling Inhibition: LY294002, a highly selective inhibitor of PI3K, was purchased from Sigma-Aldrich (St. Louis, MO, USA) and dissolved in dimethylsulfoxide (DMSO) at a stock concentration of 100 mM according to the protocol. To confirm the involvement of PI3K/Akt signaling in the exosome-mediated effects on BMSCs, the cells were placed on BLANK, SIS, SIS-EXO, and SIS–P1P2-EXO group with or without the LY294002 for 5 days. Western blotting and immunofluorescence staining was then performed as described above.

Animals and Surgical Procedures: All animal experiments were approved by the Animal Ethical and Welfare Committee of Tianjin Medical University (SYXK:2019–0004). Male six-week-old Sprague-Dawley (SD) rats were randomly divided into five groups, including blank group, SIS membrane group, SIS-EXO membrane group, Bio-Gide membrane group and SIS–P1P2-EXO membrane group. A critical size defect with a diameter of 8 mm was made on the skull with a diamond needle (Hager Meisinger Co., Ltd., Germany) under slow speed drilling. To reduce the temperature, a large amount of saline must be used for flushing, and the operation must be performed carefully to avoid damage to the dura mater and brain. The membranes were then implanted into the defect and the incision was stitched.

Micro-CT Scanning Evaluation: The rats in each group were sacrificed by isoflurane inhalation at 12 weeks postsurgery. The bone regeneration of the calvarial defect areas was evaluated by micro-CT analysis (Sky-Scan 1276, Germany). After three-dimensional (3D) visualization, the bone volume/Total volume ratio (BV/TV) and bone mineral density (BMD) were examined using CTAn software.

Histological and Immunohistochemical Analysis: After decalcification for 30 days, the tissues were embedded in paraffin and sliced (5 μm in thickness). Histological analysis was conducted by Hematoxylin Eosin (H&E) and Masson-Goldner (Solarbio, China) staining. For immunohistochemistry, the primary antibodies anti-COL1-A1 and anti-OPN (1:200 dilution; Abcam, UK) was used. The immunoreactivity was detected using fluorescence-conjugated goat anti-rabbit IgG (1:200 dilution; Solarbio, Beijing, China). The images were observed with a digital slice scanning system (Nano Zoomer, Hamamatsu, Japan).

Statistical Analysis: All the results are presented as the means ± standard deviations for each group. The date were analyzed by one-way ANOVA followed by Tukey's post hoc test. For all tests, the differences were accepted as significant if $p < 0.05$ (*).

Author statement

Shiqing Ma: Methodology, Software, Validation, Formal analysis, Investigation, Data Curation, Writing - Original Draft, Writing - Review & Editing, Visualization. Yifan Zhao: Methodology, Software, Validation, Formal analysis, Investigation, Data Curation, Writing - Original Draft, Writing - Review & Editing, Visualization. Yilin Yang: Methodology, Software, Validation, Formal analysis, Investigation, Data Curation, Writing - Original Draft, Writing - Review & Editing, Visualization. Yuzhu Mu: Formal analysis, Investigation, Visualization, Supervision. Lei Zhang: Formal analysis, Investigation, Visualization, Supervision. Jinzhe Wu: Formal analysis, Investigation, Visualization, Supervision. Rui Li: Formal analysis, Validation, Visualization, Supervision. Xiaowei Bian: Formal analysis, Validation, Visualization, Supervision. Pengfei Wei: Formal analysis, Validation, Visualization, Supervision. Wei Jing: Formal analysis, Validation, Visualization, Supervision. Bo Zhao: Conceptualization, Methodology, Formal analysis, Investigation, Writing - Original Draft, Writing - Review & Editing, Supervision, Funding acquisition. Zihao Liu: Conceptualization, Methodology, Formal analysis, Investigation, Writing - Original Draft, Writing - Review & Editing, Supervision, Funding acquisition. Jiayin Deng: Conceptualization, Methodology, Formal analysis, Investigation, Writing - Original Draft, Writing - Review & Editing, Supervision, Funding acquisition.

Declaration of competing interest

The authors declare that they have no known competing financial interests or personal relationships that could have appeared to influence the work reported in this paper.

Acknowledgements

The authors thank the funding support by the Scientific Foundation of Tianjin Education Commission (No. 2019KJ173), the Science and Technology Project of Tianjin Health Committee (No. QN20026), the Guangdong Basic and Applied Basic Research Foundation (No. 2020A1515111182), the Natural Science Foundation of Tianjin. (No. 18JCYBJC95500) and the Stomatological Hospital Project of Tianjin Medical University(No. 2020YKY06). The authors would like to thank Beijing Biosis Healing Biological Technology Co., Ltd., for supplying the SIS membranes.

Appendix A. Supplementary data

Supplementary data to this article can be found online at https://doi.org/10.1016/j.compositesb.2021.109571.

References

[1] Xie X, Cai J, Yao Y, Chen Y, Wu J, Mo X. A woven scaffold with continuous mineral gradients for tendon-to-bone tissue engineering. Compos B Eng 2021;212:1359–8368.
[2] Jung RE, Fenner N, Hämmerle CHF, Zitzmann NU. Long-term outcome of implants placed with guided bone regeneration (GBR) using resorbable and non-resorbable membranes after 12-14 years. Clin Oral Implants Res 2013;24:1065–673.
[3] Li H, Zheng J, Zhang S, Yang C, Kwon Y-D, Kim Y-J. Experiment of GBR for repair of peri-implant alveolar defects in beagle dogs. Sci Rep 2018;8(1):16532.
[4] Elgali I, Omar O, Dahlin C, Thomsen P. Guided bone regeneration: materials and biological mechanisms revisited. Eur J Oral Sci 2017;125:315–37.
[5] Bottino MC, Thomas V, Schmidt G, Vohra YK, Chu T-MG, Kowolik MJ, Janowski GM. Recent advances in the development of GTR/GBR membranes for periodontal regeneration–a materials perspective. Dent Mater 2012;28(7):703–21.
[6] Troeltzsch M, Troeltzsch M, Kauffmann P, Gruber R, Brockmeyer P, Moser N, Rau A, Schliephake H. Clinical efficacy of grafting materials in alveolar ridge augmentation: a systematic review. J Cranio-Maxillo-Fac Surg 2016;44(10):1618–29.
[7] Guda T, Walker JA, Singleton BM, Hernandez JW, Son J-S, Kim S-G, Oh DS, Appleford MR, Ong JL, Wenke JC. Guided bone regeneration in long-bone defects with a structural hydroxyapatite graft and collagen membrane. Tissue Eng 2013;19(17–18):1879–88.
[8] Elgali I, Turri A, Xia W, Norlindh B, Johansson A, Dahlin C, Thomsen P, Omar O. Guided bone regeneration using resorbable membrane and different bone substitutes: early histological and molecular events. Acta Biomater 2016:409–23.
[9] Piao Z-G, Kim J-S, Son J-S, Lee S-Y, Fang X-H, Oh J-S, You J-S, Kim S-G. Osteogenic evaluation of collagen membrane containing drug-loaded polymeric microparticles in a rat calvarial defect model. Tissue Eng 2014;20(23–24):3322–31.
[10] Xu C, Lei C, Meng L, Wang C, Song Y. Chitosan as a barrier membrane material in periodontal tissue regeneration. J Biomed Mater Res B Appl Biomater 2012;100(5):1435–43.

[11] Yi S, Ding F, Gong L, Gu X. Extracellular matrix scaffolds for tissue engineering and regenerative medicine. Curr Stem Cell Res Ther 2017;12(3):233–46.
[12] Turri A, Elgali I, Vazirisani F, Johansson A, Emanuelsson L, Dahlin C, Thomsen P, Omar O. Guided bone regeneration is promoted by the molecular events in the membrane compartment. Biomaterials 2016;84:167–83.
[13] Hodde JP, Badylak SF, Brightman AO, Voytik-Harbin SL. Glycosaminoglycan content of small intestinal submucosa: a bioscaffold for tissue replacement. Tissue Eng 1996;2(3):209–17.
[14] Lin X, Robinson M, Petrie T, Spandler V, Boyd WD, Sondergaard CS. Small intestinal submucosa-derived extracellular matrix bioscaffold significantly enhances angiogenic factor secretion from human mesenchymal stromal cells. Stem Cell Res Ther 2015;6(1):164.
[15] Zhao P, Li X, Fang Q, Wang F, Ao Q, Wang X, Tian X, Tong H, Bai S, Fan J. Surface modification of small intestine submucosa in tissue engineering. Regener Biomater 2020;7(4):339–48.
[16] Li M, Zhang C, Cheng M, Gu Q, Zhao J. Small intestinal submucosa: a potential osteoconductive and osteoinductive biomaterial for bone tissue engineering. Mater Sci Eng C Mater Biol Appl 2017;75:149–56.
[17] Won J-E, Yun Y-R, Jang J-H, Yang S-H, Kim J-H, Chrzanowski W, Wall IB, Knowles JC, Kim H-W. Multifunctional and stable bone mimic proteinaceous matrix for bone tissue engineering. Biomaterials 2015;56:46–57.
[18] Deng A, Chen A, Wang S, Li Y, Liu Y, Cheng X, Zhao Z, Lin D. Porous nanostructured poly- l -lactide scaffolds prepared by phase inversion using supercritical CO_2 as a nonsolvent in the presence of ammonium bicarbonate particles. J Supercrit Fluids 2013;77:110–6.
[19] Chen K-Y, Liao W-J, Kuo S-M, Tsai F-J, Chen Y-S, Huang C-Y, Yao C-H. Asymmetric chitosan membrane containing collagen I nanospheres for skin tissue engineering. Biomacromolecules 2009;10(6):1642–9.
[20] Zhang K, Zhao X, Chen X, Wei Y, Du W, Wang Y, Liu L, Zhao W, Han Z, Kong D, Zhao Q, Guo Z, Han Z, Liu N, Ma F, Li Z. Enhanced therapeutic effects of mesenchymal stem cell-derived exosomes with an injectable hydrogel for hindlimb ischemia treatment. ACS Appl Mater Interfaces 2018;10(36):30081–91.
[21] Phinney DG, Pittenger MF. Concise review: MSC-derived exosomes for cell-free therapy. Stem Cell 2017;35(4):851–8.
[22] Li W, Liu Y, Zhang P, Tang Y, Zhou M, Jiang W, Zhang X, Wu G, Zhou Y. Tissue-engineered bone immobilized with human adipose stem cells-derived exosomes promotes bone regeneration. ACS Appl Mater Interfaces 2018;10(6):5240–54.
[23] Desdín-Micó G, Mittelbrunn M. Role of exosomes in the protection of cellular homeostasis. Cell Adhes Migrat 2017;11(2):127–34.
[24] Zhang C, Liu L-H, Qiu W-X, Zhang Y-H, Song W, Zhang L, Wang S-B, Zhang X-Z. A transformable chimeric peptide for cell encapsulation to overcome multidrug resistance. Small 2018;14(11):e1703321.
[25] Liu Z, Ma S, Duan S, Xuliang D, Sun Y, Zhang X, Xu X, Guan B, Wang C, Hu M, Qi X, Zhang X, Gao P. Modification of titanium substrates with chimeric peptides comprising antimicrobial and titanium-binding motifs connected by linkers to inhibit biofilm formation. ACS Appl Mater Interfaces 2016;8(8):5124–36.
[26] Takagi J, Asai H, Saito Y. A collagen/gelatin-binding decapeptide derived from bovine propolypeptide of von Willebrand factor. Biochemistry 1992;31(36):8530–4.
[27] Wahyudi H, Reynolds AA, Li Y, Owen SC, Yu SM. Targeting collagen for diagnostic imaging and therapeutic delivery. J Contr Release 2016;240:323–31.
[28] Badylak SF, Record R, Lindberg K, Hodde J, Park K. Small intestinal submucosa: a substrate for in vitro cell growth. J Biomater Sci Polym Ed 1998;9(8):863–78.
[29] Xu Q, Shanti RM, Zhang Q, Cannady Jr SB, OM BW, Le AD. A gingiva-derived mesenchymal stem cell-laden porcine small intestinal submucosa extracellular matrix construct promotes myomucosal regeneration of the tongue. Tissue Eng 2017;23(7–8):301–12.
[30] Gao X, Ran N, Dong X, Zuo B, Yang R, Zhou Q, Moulton HM, Seow Y, Yin H. Anchor peptide captures, targets, and loads exosomes of diverse origins for diagnostics and therapy. Sci Transl Med 2018;10(444):eaat0195.
[31] Chen X, Zaro JL, Shen W-C. Fusion protein linkers: property, design and functionality. Adv Drug Deliv Rev 2013;65(10):1357–69.
[32] Wen D, Foley SF, Hronowski XL, Gu S, Meier W. Discovery and investigation of O-xylosylation in engineered proteins containing a (GGGGS)n linker. Anal Chem 2013;85(9):4805–12.
[33] Ma S, Chen Z, Qiao F, Sun Y, Yang X, Deng X, Cen L, Cai Q, Wu M, Zhang X, Gao P. Guided bone regeneration with tripolyphosphate cross-linked asymmetric chitosan membrane. J Dent 2014;42(12):1603–12.
[34] Keshtkar S, Azarpira N, Ghahremani MH. Mesenchymal stem cell-derived extracellular vesicles: novel frontiers in regenerative medicine. Stem Cell Res Ther 2018;9(1):63.
[35] Salhotra A, Shah HN, Levi B, Longaker MT. Mechanisms of bone development and repair. Nat Rev Mol Cell Biol 2020;21(11):696–711.
[36] Chen Y, Udduttula A, Xie X, Zhou M, Sheng W, Yu F, Weng J, Wang D, Teng B, Manivasagam G, Zhang J, Ren P, Kang B, Zeng H. A novel photocrosslinked phosphate functionalized Chitosan-Sr5(PO4)2SiO4 composite hydrogels and in vitro biomineralization, osteogenesis, angiogenesis for bone regeneration application. Compos B Eng 2021;222:1359–8368.
[37] Zhang B, Wang M, Gong A, Zhang X, Wu X, Zhu Y, Shi H, Wu L, Zhu W, Qian H, Xu W. HucMSC-exosome mediated-wnt4 signaling is required for cutaneous wound healing. Stem Cell 2015;33(7):2158–68.
[38] Zhang J, Liu X, Li H, Chen C, Hu B, Niu X, Li Q, Zhao B, Xie Z, Wang Y. Exosomes/tricalcium phosphate combination scaffolds can enhance bone regeneration by activating the PI3K/Akt signaling pathway. Stem Cell Res Ther 2016;7(1):136.